Received: 5 December 2023 | Accepted: 24 May 2024 | Published online: 29 June 2024

DOI: 10.1002/agj2.21630

Agronomy Journal

ORIGINAL ARTICLE

Agronomy, Soils, and Environmental Quality

Reformulation of dicamba herbicide: Impacts on offsite transport and soybean damage

Caleb R. Hammer[1] | Timothy J. Griffis[1] | John M. Baker[1,2] | Pamela J. Rice[1,2] | Lara E. Frankson[2] | Jeffrey L. Gunsolus[3] | Matthew D. Erickson[1] | Ke Xiao[1] | Aarti P. Mistry[1] | Debalin Sarangi[3]

[1]Department of Soil, Water, and Climate, University of Minnesota, Saint Paul, Minnesota, USA

[2]Soil and Water Management Research Unit, USDA-ARS, Saint Paul, Minnesota, USA

[3]Department of Agronomy and Plant Genetics, University of Minnesota, Saint Paul, Minnesota, USA

Correspondence
Caleb R. Hammer and Timothy J. Griffis, Department of Soil, Water, and Climate, University of Minnesota, Saint Paul, MN 55108, USA.
Email: Hamme785@umn.edu and timgriffis@umn.edu

Assigned to Associate Editor Albert Adjesiwor.

Funding information
University of Minnesota Rapid Agricultural Response Fund; Minnesota Department of Agriculture; USDA Agricultural Research Service; US Department of Energy AmeriFlux Core Site Program

Abstract

The herbicide dicamba (3,6-dichloro-2-methoxybenzoic acid) is commonly used to control broadleaf weeds in soybeans. Dicamba, however, is susceptible to volatilization and drift, thereby causing significant plant damage to nontarget crops downwind. Dicamba was reformulated to reduce volatility and off-target movement. The effectiveness of the dicamba reformulation was assessed by quantifying dicamba emissions following spray application and investigated how meteorological factors influenced the off-target movement. The experiments were conducted at the University of Minnesota Agricultural Experiment Station (UMORE Park) during the growing season of 2018, 2019, 2021, and 2022. Multiple high-flow polyurethane foam air samplers were used to measure dicamba concentrations downwind from a 4-ha soybean field sprayed with dicamba. Dicamba emissions were estimated using backward Lagrangian modeling constrained by the air sample observations. The results indicate that dicamba emissions and downwind transport were significant for several days following application. Further, non-traited soybeans located within 15–45 m showed substantial dicamba-related damage. In warmer, drier seasons, increased dicamba emissions caused more severe damage to downwind soybeans, likely worsened by drought stress preventing recovery. Favorable atmospheric conditions that reduced potential drift can be difficult to achieve in terms of the typical weather experienced over agricultural sites in the Upper Midwest. These results indicate that the dicamba reformulation has not adequately prevented significant post-spray volatilization losses and downwind transport.

Abbreviations: BAPMA, *N*, *N*-bis-(3-aminopropyl) methylamine; bLS, backward Lagrangian stochastic; DGA, diglycloamine; EPA, Environmental Protection Agency; fLS, forward Lagrangian stochastic; LC, liquid chromatography; PUF, polyurethane foam; RSD, relative standard deviation.

1 INTRODUCTION

Dicamba (3,6-dichloro-2-methoxybenzoic acid) is a group 4 herbicide, a class of chemicals that bind to plant receptors for auxin or indoleacetic acid, resulting in stunting the plant's growth and, ultimately, killing the plant (M. R. Behrens et al., 2007; Hartzler, 2017a). Dicamba has a relatively short half-life of about 14 days and can stay in the soil longer than other group 4 herbicides, with an average half-life of 6 days (Hartzler, 2017a). Dicamba's longer half-life, effectiveness, and availability created an advantage in the agricultural market and an effective herbicide for broadleaf plants and weed control. However, its use has resulted in damage to neighboring susceptible crop fields due to drift (i.e., offsite transport during application), volatilization (i.e., evaporation after application), and downwind transport causing damage to nontarget crops (Riter et al., 2020). Dicamba was first approved for agricultural systems in 1962, and by 1971, a total of ∼25,854 kg of dicamba was applied to crops in Minnesota, Wisconsin, and Michigan (Andrilenas, 1974). However, as new herbicides became available, farmers preferred to use other less volatile broad-spectrum herbicides such as glyphosate (Hartzler, 2017b; Zaccaro-Gruener et al., 2022).

The renewed interest in applying dicamba to soybean (*Glycine max*) crops resulted from weed pressure due to increased resistance to other herbicides such as glyphosate (Batts et al., 2021). Recently, dicamba use in soybeans has increased due to herbicide-resistant weeds and the development of dicamba-resistant (traited) soybeans. The dicamba reformulation approved by the United States Environmental Protection Agency (EPA) used *N*, *N*-Bis-(3-aminopropyl) methylamine (BAPMA) salt or diglycloamine (DGA) salt to reduce volatility and combat weeds that had become resistant to glyphosate (Batts et al., 2021). Dicamba with BAPMA reduces the boiling point and vapor pressure of the salt, reducing the overall volatility (Riter et al., 2021). The DGA formulation removes the volatile dimethylamine to reduce the vaporization problem (Riter et al., 2021). When dicamba attaches to free hydrogen molecules, it is more likely to volatilize, leading to a greater chance of vapor or particle drift onto nontarget crops, especially when applied as a spray (DaSilva et al., 2006; Hartzler, 2017a). With the reformulation, agrochemical companies recommended that farmers add pH and volatilization buffers to reduce drift and volatilization. For example, the dicamba formulation XtendiMax can be mixed with the additive VaporGrip Technology to reduce volatilization by decreasing the amount of dicamba molecules combined with free hydrogen molecules (MDA, 2019).

Non-traited soybeans are at relatively high risk of injury from offsite dicamba movement, with most reported dicamba damage cases involving soybean (EPA, 2023). Symptoms of dicamba spray drift and volatilization on neighboring plants include stem twisting, yellowing of leaves, leaf wrinkling/crinkling, leaf loss, reduction in plant height, physical deformities, flower reduction and, in some cases, plant death (Castner et al., 2022; Marques et al., 2021; McCown et al., 2018; Riter et al., 2020; Robinson et al., 2013; Sciumbato et al., 2004). These symptoms can lead to yield and profit loss in the agricultural industry (Batts et al., 2021; McCown et al., 2018; Meyeres et al., 2021, 2022).

Core Ideas

- Dicamba herbicide drift and volatilization harms nearby crops, despite new formulations and label requirements.
- Dicamba emissions and drift were estimated using polyurethane foam air samplers and Lagrangian modeling.
- Dicamba was detected downwind up to 4 days post application.
- Dicamba-related damage to nontarget crops was exacerbated during hotter and drier conditions.

Despite new dicamba formulations, the ongoing challenges continue to persist in soybean production areas worldwide (M. Bish et al., 2021; M. D. Bish, Farrell, et al., 2019; Egan & Mortensen, 2012; Riter et al., 2020, 2021; Sall et al., 2020). Globally, countries adopt different strategies to address these challenges. For example, Brazil deregulated soybeans tolerant to herbicides like dicamba and glyphosate, but limited dicamba use to preplanting to prevent adverse environmental impacts (Carbonari et al., 2022). Other countries such as Canada and the United States have regulated dicamba application through measures like buffer zones to mitigate water contamination and to protect endangered species (EPA, 2022; Government of Canada, 2022).

In the United States, six major soybean production states of the Upper Midwest including Illinois, Indiana, Iowa, Michigan, Minnesota, and Wisconsin, in collaboration with the EPA, are developing regulations aimed at minimizing off-target movement and subsequent damage to neighboring crops. These regulations include the establishment of application cut-off dates, for example, before June 12 in southern Minnesota and before June 30 in northern Minnesota, as defined by the I-94 highway (EPA, 2022; IDOA, 2024; Jha, 2023; MDA, 2019; MDARD, 2024; OISC, 2023; Tomasko, 2022). Additionally, Minnesota and Illinois have introduced further requirements for state-approved dicamba applications, such as enforcing a maximum temperature of 29.4°C, the use of an approved pH buffering product, and a downwind buffer zone of 73–94 m in areas where endangered species are present. Minnesota is noted for having the most rigorous regulations, requiring record keeping of application information and additional application cutoffs for Xtendimax, which must be applied before the V4 growth stage (MDA, 2019). However, in 2021, a total of 1726 instances of damage were officially reported in the Upper Midwest, impacting over 15.52 million ha of soybeans across six states (EPA, 2022; MDA, 2019).

Multiple meteorological and environmental factors can impact the volatilization and transport of dicamba. However, the factors influencing the transport and extent of offsite transport are poorly constrained because atmospheric observations at the time of application are typically not made. There is considerable concern and debate regarding dicamba's drift potential, volatility, atmospheric loading, and subsequent transport to nontarget fields and natural ecosystems (Jones et al., 2019; Riter et al., 2020; Soltani et al., 2020). Environmental variables including air temperature, dew point, wind speed, and atmospheric stability have been identified as key factors associated with increased volatilization and drift. Warm temperatures can increase dicamba volatilization and stable atmospheric conditions can lead to an increase in off-target drift (M. D. Bish, Farrell, et al., 2019; M. D. Bish, Guinan, et al., 2019; Egan & Mortensen, 2012; Grint & Werle, 2021; Mueller & Steckel, 2021). Understanding which meteorological and environmental factors influence volatility and offsite movement could significantly improve best management practices for dicamba application.

Here, we present data and analyses from four experiments conducted in Minnesota over the period 2018–2019 and 2021–2022 to investigate dicamba volatilization and downwind transport following application to soybean crops. The objectives of this study were to (1) measure dicamba concentrations in the atmosphere downwind of application sites, (2) quantify dicamba loss and off-site transport using a combination of air sample observations and Lagrangian atmospheric transport modeling, and (3) provide informed estimates of potential downwind transport based on meteorological conditions.

2 | METHODOLOGY

2.1 | Field site

This study was conducted at UMORE Park, University of Minnesota, near Rosemount, MN (44˚43′18.37″ N, 93˚06′46.14″ W). The experimental field site is shown in Figure 1. In each of the 4 years, diglycolamine salt of dicamba (3,6-dichlor-o-anisic acid) with XtendiMax and VaporGrip (Bayer CropScience LP) Technology was applied as a spray using a John Deere 4045 Self-Propelled Sprayer with a boom height of 0.61 m and width of 36.58 m during the morning hours of June to traited soybean. Soybean growth stages at the time of application ranged from V1–V3 over the 4-year period. Dicamba was applied to the traited soybean at label rates (0.56 kg ha^{-1}) each year.

Air sampling for dicamba was conducted near-continuously for a period of 5 days each year in June 2018, 2019, 2021, and 2022. On day 0 (prior to spray), we measured ambient air to establish "background" dicamba concentrations. Spray application (day 1) was characterized by spray drift and subsequent volatilization, while post-application (day 2–4) included only volatilization. At the field site, 4.05 ha of dicamba-resistant (traited) soybeans (Golden Harvest 1486X [2018–2019], Golden Harvest 1414X [2021], and Golden Harvest 1442XF [2022]) were planted and 16.2 ha of non-dicamba-resistant (non-traited) soybeans (NK S14-A6 [2018–2019], Pioneer 16T85E [2021], and Golden Harvest 0842E3 and Golden Harvest 1472E3 [2022]) were planted with 0.76-m spaced rows (Figure 1). The experimental design allowed assessment of downwind transport of dicamba in air using high-flow air samplers (described below) as well as soybean plant damage (described below) associated with offsite transport.

2.2 | Air quality monitoring and meteorological measurements

Air sampling and meteorological equipment were located in adjacent off-target non-traited soybean fields. Tisch air samplers (TE-1000 high volume PUF sampler, Tisch Environmental) were used to monitor the offsite movement of dicamba. The Tisch sampler intakes were located 1.2 m above the soil surface and continuously collected air samples for a period of about 24 h. Air was pulled through filter paper (SKU TE-QMA4, Tisch Environmental) followed by a large polyurethane foam (PUF) and then small (one-third section of the large PUF) PUF cylinder (24295; Restek [2018–2021], P226131C; SKC Inc [2022]) at approximately 280 L min^{-1}. The PUFs and filter papers were replaced approximately every 24 h. To prevent contamination of the filter papers and PUFs, prior to deployment and following collection, all field personnel wore clean surgical gloves and the PUFs and filter papers were wrapped in solvent-rinsed foil. Following collection, all samples were stored at −40˚C prior to lab extraction.

In 2018, seven Tisch samplers were used to monitor dicamba concentrations from the dominant wind directions during the experiment, resulting in a total of 147 samples collected (Figure 2). From day 0 (i.e., prior to spray application) to day 2, six samplers were positioned north of the traited soybean plot, while one sampler was placed south of the plot, approximately 10, 25, and 50 m north of the plot's edge, and 25 m south. On day 3, five samplers were located to the north and two to the south at distances of 25 and 50 m. On day 4, four samplers were placed to the north, one sampler was positioned

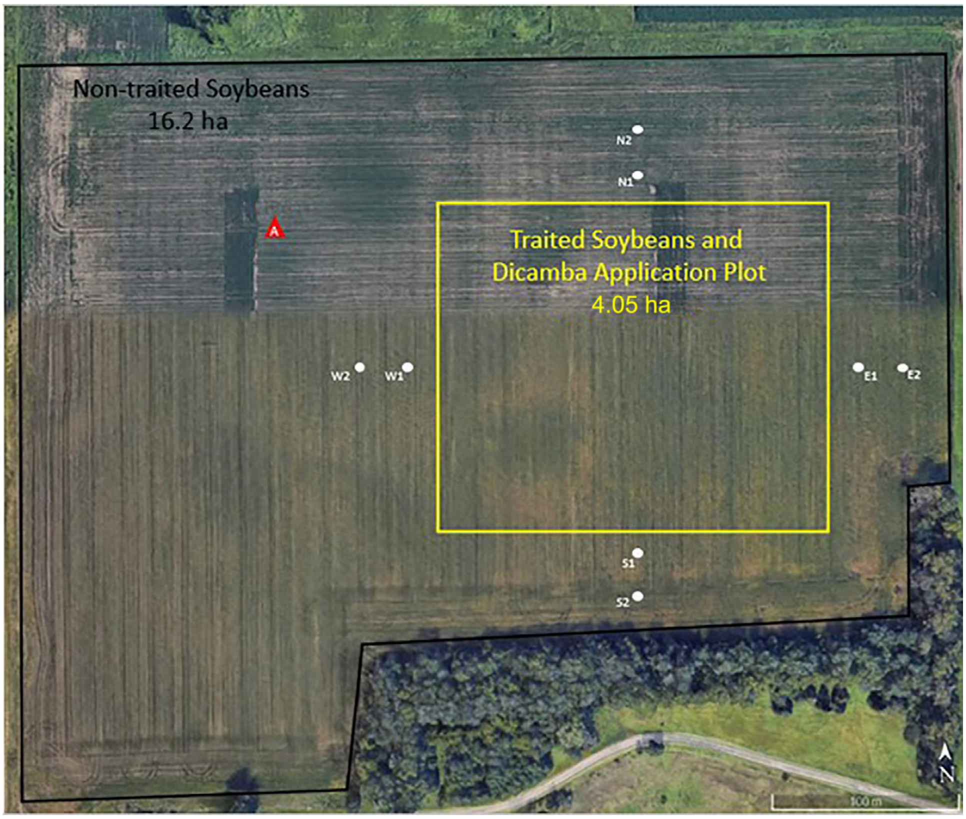

FIGURE 1 Air sampler locations (2019, 2021, and 2022). Non-traited and traited fields were 16.2 and 4.05 ha, respectively. Air samples were taken 1.2 m above the soil surface. Samplers north 1 [N1], east 1 [E1], south 1 [S1], and west 1 [W1] were located 12 m from the traited plot; north 2 [N2], east 2[E2], south 2 [S2], and west 2 [W2] were located 40 m away from the traited plot. The meteorological tower [A] was instrumented with a sonic anemometer, air temperature, humidity, and radiation sensors.

10 m within the traited plot, and two samplers were situated south of the plot. The northern samplers were positioned 80 m from the nearest corner of the traited plot, and the southern samplers were centered between the traited plot corners. In 2019, 2021, and 2022, two Tisch samplers were deployed in each cardinal direction (north 1 [N1], north 2 [N2], south 1 [S1], south 2 [S2], east 1 [E1], east 2 [E2], west 1 [W1], and west 2 [W2]) in the off-target soybean field, centered between the corners of the dicamba traited plot at distances of 12 and 40 m from the edge of the dicamba traited plot (Figure 1). A total of 150 samples were collected in 2019, 132 samples in 2021, and 160 samples in 2022.

An eddy covariance system was deployed at the dicamba field site and at other nearby sites (within 3 km) at UMORE Park as part of the AmeriFlux program (Baker & Griffis, 2005). These systems were used to measure key meteorological variables including wind speed, wind direction, air temperature, relative humidity, water vapor mixing ratio, atmospheric stability, friction velocity, latent and sensible heat fluxes, and net radiation balance.

The Monin–Obukhov atmospheric stability was estimated from the potential virtual temperature, friction velocity, and turbulent heat flux (Huang & Li, 2023; Oke, 1987; Stull, 1988). The turbulent momentum and thermal fluxes, characterized by friction velocity and turbulent heat flux, are key indicators of atmospheric stability. A stable atmosphere tends to suppress vertical motions and reduces turbulence intensity and diffusion. In contrast, unstable atmospheric conditions promote vertical motions and diffusion. Stability values near zero indicate neutral atmospheric stability, whereas negative and positive values are classified as unstable and stable conditions, respectively.

2.3 | Extraction of dicamba from filter paper and PUFs

Dicamba was extracted from the PUFs, and filter papers in a lab located at the University of Minnesota, Saint Paul Campus. First, the samples were removed from the freezer and warmed to room temperature over a period of 45 min. Filter paper samples were submerged in 25 mL of 10 ng mL^{-1} d3-dicamba in methanol and then placed on a shaker (Thermolyne Bigger Bill, M49235) at 150 rpm for 60 min, flipping them over halfway through. The extract was filtered through a 0.45 µm polytetrafluoroethylene syringe filter (Fisherbrand,

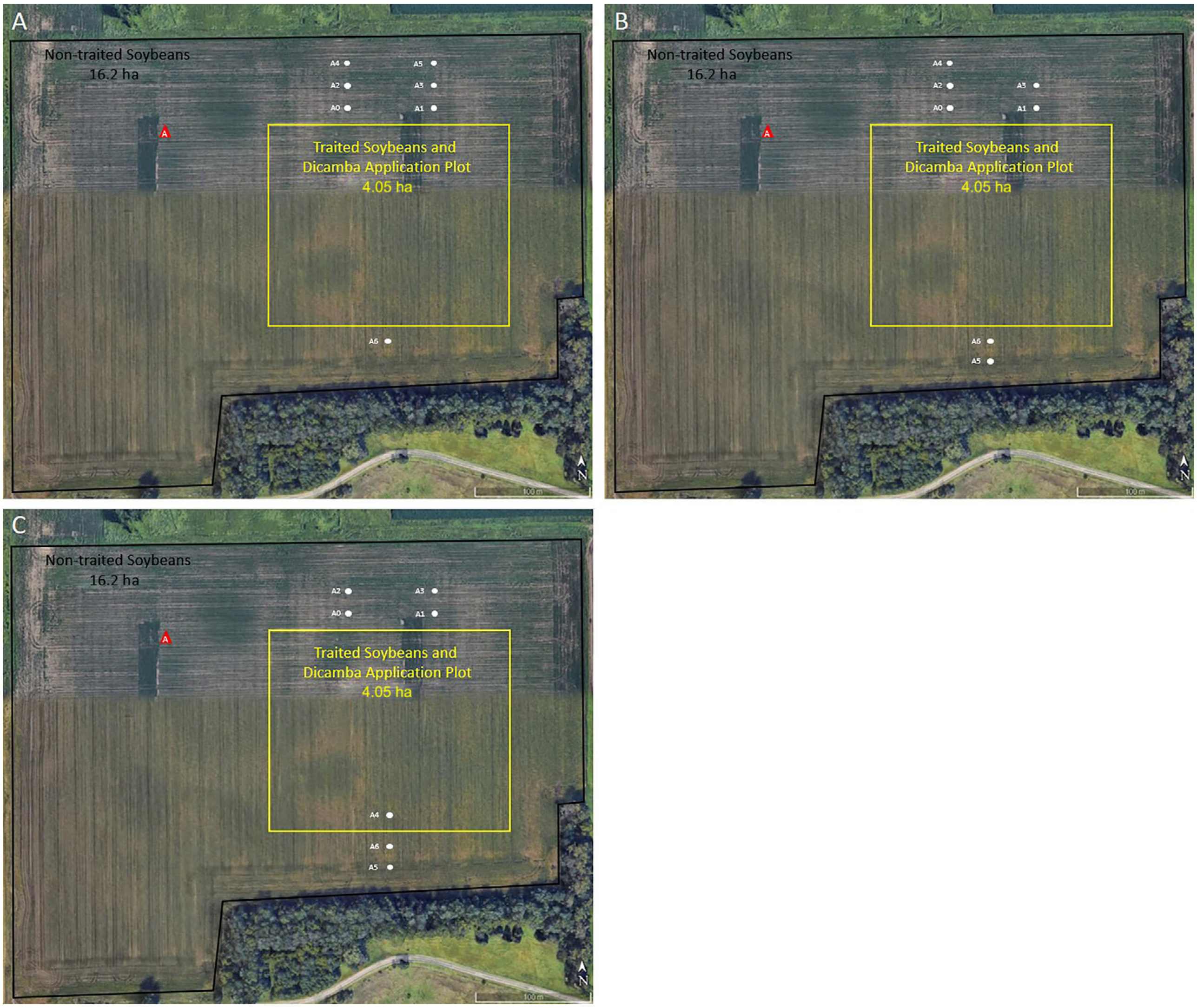

FIGURE 2 Location of air samplers in 2018. (A) Day 0–2; A0, A1: 10 m; A2, A3: 25 m; A4, A5: 50 m north; and A6: 25 m south of traited plot. (B) Day 3; A0, A1: 10 m; A2, A3: 25 m north; A4: 50 m north; A5: 50 m; and A6: 25 m south. (C) Day 4; A0, A1: 10 m; A2, A3: 25 m north; A4: within 10 m; A5: 50 m; and A6: 25 m south of the traited plot. Meteorological tower [A] was instrumented with a sonic anemometer, air temperature, humidity, and radiation sensors.

09-719H) into a liquid chromatography (LC) vial. The LC vials were analyzed on a liquid chromatograph with tandem mass spectrometer (Shimadzu LC-40D with Sciex 5500+ MSMS).

The liquid chromatography tandem mass spectrometry method was adapted from Riter et al. (2020). An Agilent InfinityLab Poroshell 120 EC-C18 (4.6 × 100 mm, 27 micron) column, held at 50˚C, was used to separate analytes. The method was run on a Sciex LC40 HPLC with a Sciex 5500+ MSMS. Mobile phase A consisted of 0.02% formic acid in water and mobile phase B consisted of 0.02% formic acid in methanol. The mobile phase gradient is provided in Table S1. Each sample injection was 50 µL with a 50%:50% methanol: water needle rinse before and after each injection. The MSMS was set at electrospray ionization negative mode with the curtain gas set at 50.0 psi, collision gas at 7 psi, ion spray voltage at −2500 V, temperature set at 500˚C, and ion source gases 1 and 2 set at 40.0 psi. The multiple reaction monitoring transitions and parameters used to monitor dicamba and the internal standard dicamba-d3 are described in Table S2. PUFs were extracted and analyzed in the same manner as the filter paper except 400 mL of 10 ng mL^{-1} d3-dicamba in methanol was used to extract and the PUFs were shaken for 90 min. Additionally, one blank and one control spike (spiked with 75 ng of dicamba) was extracted approximately every 15 samples.

The mean recoveries for filter paper, small PUFs, and large PUFs consistently fell within the acceptable range of 70%–120%, with a relative standard deviation (RSD) of equal to or less than 20%, as specified by the EPA (EPA, 2017). The average recovery efficiency for filter paper across all years stood at approximately 102.87% ± 8.64%, with an RSD of 8.5%. For large PUFs, the mean recovery efficiency across all years was approximately 88.7% ± 14.8%, with an RSD of 16.6%. Correspondingly, the mean recovery efficiency for small PUFs for all years was roughly 98.9% ± 12.5%, accompanied by an RSD of 12.7%. Dicamba concentrations reported in this study are the sum of the filter paper, large PUF, and small PUF for each sampler.

2.4 | Plant symptomology

To detect the biophysical effects of offsite dicamba movement, independent of the atmospheric monitoring, we used visual symptomology indicators (Ritter et al., 2021) for the non-traited soybean plots. Plants were inspected for damage such as stem twisting and leaf cupping. A small cluster of soybeans was photographed and recorded 1 week post-spray application for five consecutive weeks. The inspection was conducted in the four cardinal directions at 15, 30, and 45 m in the non-traited soybean. Symptoms were rated on a scale ranging from 0 to 5. Dicamba damage rated at 0 signified no effect on soybean plants from the dicamba application. A 1 rating corresponded to slight leaf crinkling and stem twisting at the leaflets of the terminal leaf and second leaf of the soybean plant, and the soybean growth rate was normal. A 2 rating indicated moderate leaf cupping and stem twisting on the terminal with suppression of expansion of the terminal leaf. A 3 rating was visible deformation of the soybean plant leaves with reduced growth of axillary leaves and malformation of terminal leaves, leading to leaves less than half of the size of traited soybean. A 4 rating was severe deformation and death of portions of the soybean plant with slight terminal growth, terminal bud death, and chlorosis and necrosis in axillary leaf clusters. A 5 rating was the death of the soybean plant. Recovery of the soybean plant is possible for a dicamba damage rating of 0–3 (Dintelmann et al., 2022; Foster & Griffen, 2018; McCown et al., 2018; Robinson et al., 2013), but soybean plants are unlikely to recover from a dicamba damage rating of 4. See Figure 3 showing plant symptomology scale description and photos.

2.5 | Constraining dicamba emissions and downwind transport

To constrain dicamba emissions and downwind transport, we used the Lagrangian stochastic model WindTrax (V.2.0.9.6, 2011, Thunder Beach Scientific). WindTrax has been applied in numerous micrometeorological applications including pesticide transport problems (Flesch et al., 2002; T. K. Flesch & Wilson, 2015; Prueger & Kustas, 2015). We used the backward Lagrangian stochastic (bLS) model in combination with our dicamba air concentration measurements and meteorological forcing data (i.e., atmospheric stability, wind direction, wind speed, and air temperature) to constrain dicamba emissions from the traited soybean field. The dicamba emissions (units: ng m^{-2} s^{-1}) and uncertainties were simulated for each day following spray application.

The forward Lagrangian stochastic (fLS) model was used to estimate the downwind concentration of dicamba (unit: ng m^{-3}) and to assess the influence of atmospheric stability on downwind transport. In these numerical experiments, concentration observations were used to constrain the modeled downwind concentration estimates. Here, we placed "virtual" sensors within the model domain at 25, 50, 75, and 100 m away from the edge of the traited soybean field to capture the downwind concentrations (Figures S1 and S2). Dicamba concentrations, mean air temperature, atmospheric stability, average wind speed, and wind direction from day 2 of 2021 and 2022 were used in the model to predict the downwind transport of dicamba for seven different atmospheric stabilities: very unstable, moderately unstable, slightly unstable, neutral, slightly stable, moderately stable, and very stable.

2.6 | Statistical analyses

All meteorological and concentration data were analyzed using software R version 4.2.1 (R Core Team, 2021). The daily and annual averages of air temperature, wind speed, wind direction, friction velocity, relative humidity, water vapor concentration, atmospheric pressure, and vapor pressure deficit, along with the median atmospheric stability, were analyzed. Pearson correlation, one-way analysis of variance (ANOVA), and linear regression analyses were employed to assess the statistical relation between meteorological variables and dicamba concentration and dicamba flux. In the ANOVA analyses, the raw dicamba concentration, dicamba flux, and meteorological variables were assessed for normality using the Shapiro–Wilk test and power transformed to satisfy the homogeneity and normality assumptions (Balkema & Pancheva, 2016; Shapiro & Wilk, 1965).

3 | RESULTS AND DISCUSSION

3.1 | Weather, climate, and plant growth

The key differences in weather and climate parameters among the study periods are described below. First, we characterize the spring (April–May) antecedent climate prior to the dicamba experiments that were conducted in June. Spring 2018 was the warmest (median air temperature, 12.0°C) and driest (total precipitation, 148 mm) of the experimental years.

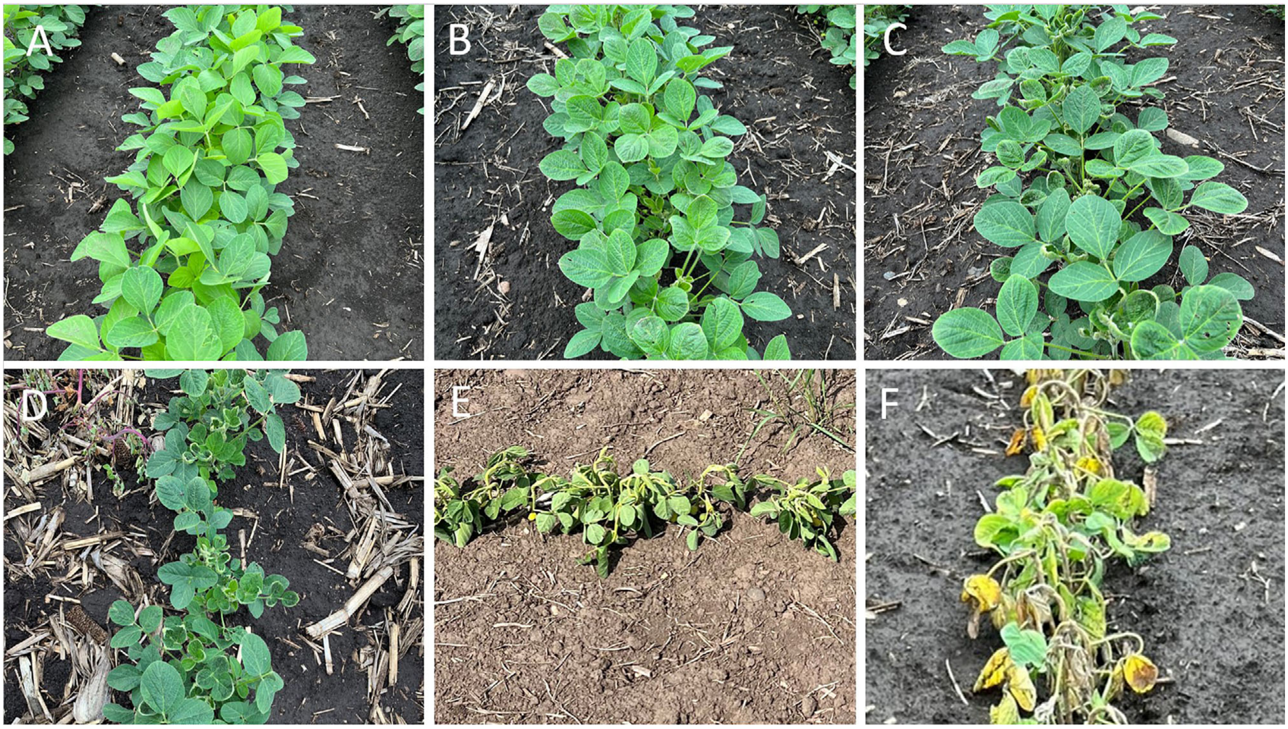

FIGURE 3 Dicamba physical damage assessment. (A) level 0: no damage, (B) level 1: minor damage, (C) level 2: moderate damage, (D) level 3: moderately severe damage, (E) level 4: near death, and (F) level 5: death.

Spring 2019 was relatively cool (8.9˚C) and wet (282 mm). Spring 2021 was similar to 2018 with a median air temperature of 11.1˚C and total precipitation of 142 mm. Finally, spring 2022 was relatively cold (8.9˚C) and wet (200 mm). These spring conditions influenced the planting dates and soybean phenology and growth patterns. In 2018, soybean planting commenced on May 18, while in 2019, it was initiated on June 1. Similarly, in 2021 and 2022, the soybeans were planted on June 2 and June 3, respectively. Notably, during the growing seasons of 2018 and 2021, the soybeans exhibited a typical growth trajectory and healthy canopy development. Conversely, the 2019 growing season witnessed a diminished growth rate, resulting in stunted plants later in the season, leading to reduced canopy coverage. The 2022 growing season was characterized by a slower growth rate relative to 2018. However, by the end of the 2022 growing season, the soybean canopy had recovered and exhibited increased biomass, surpassing that of 2018.

In 2018, dicamba was applied on June 14 at 9:00 a.m. to V2 soybeans under southeasterly winds at 4.5 m s^{-1} and slightly unstable atmospheric conditions ($z/L = -0.04$). In 2019, the application took place on June 17 at 10:30 a.m. for V1 and V2 soybeans, with a southerly wind of 1.8 m s^{-1} in unstable conditions ($z/L = -0.4$). The 2021 application occurred on June 23 at 12:00 p.m. for V2 soybeans, featuring a southeast wind of 2.2 m s^{-1} under unstable conditions ($z/L = -0.1$). Finally, in 2022, dicamba was applied on June 27 at 10:00 a.m. to V2 and V3 soybeans with a south wind of 1.5 m s^{-1} under unstable conditions ($z/L = -0.3$).

In summary, Table 1 highlights the key climatic differences among the experimental periods. These differences include warm and wet conditions in 2018, markedly cooler conditions in 2019, and drought-like conditions in 2022.

3.2 | Plant symptomology

The non-traited soybean plants in the field showed visible signs of dicamba damage (Figure 3) after 1 week of spray application, supporting that there was significant offsite transport. The daily meteorological conditions of each year are shown in Table 2 and Figure S3a–d.

In 2018, during the first week (June 29, 2018) assessment, the dicamba plant damage was minor in the south and west at 15 and 30 m, and no plant damage was detected at 45 m. In the north and east, there was no plant damage detected. The second assessment (July 2, 2018) showed level 3 damage in the north and south, level 2 damage in the west, and level 1 damage in the east. The third assessment (July 6, 2018) showed level 2 damage in the north, level 1 damage in the south and west, and no damage in the east. The final assessment (July 25, 2018) showed level 1 damage in the north, south, and east. In 2018, the onsite prevailing wind direction correlated with the observed dicamba damage in the north direction in

TABLE 1 Climate summary for the dicamba experimental periods.

	Mean temperature (°C)			Maximum temperature (°C)			Minimum temperature (°C)			
Experimental period	**Daily**	**Daytime**	**Nighttime**	**Daily**	**Daytime**	**Nighttime**	**Daily**	**Daytime**	**Nighttime**	**Precipitation (mm)**
June 13 to June 18, 2018	22.4	26.0	22.4	32.7	32.7	30.2	15.0	19.4	15.2	103.6
June 14 to June 21, 2019	18.4	20.4	16.2	27.7	27.7	22.5	10.8	13.6	10.8	19.7
June 22 to June 28, 2021	22.1	24.8	19.9	31.4	31.4	28.6	12.2	18.1	12.2	23.3
June 22 to July 1, 2022	22.0	24.7	30.4	31.3	31.3	30.8	10.7	16.6	10.7	3.3

the non-traited field. The dicamba concentrations measured by the Tisch samplers (described below) were also highest in the north and west.

In 2019, during the first week (July 2, 2019) assessment, the dicamba damage was level 1 in all directions. The second week (July 8, 2019) showed level 2 damage in the north, east, and west and level 1 damage in the south. During the third week (July 27, 2019), dicamba damage was level 2 in all directions. In 2019, the onsite prevailing wind direction correlated with the observed dicamba damage in the northeast direction in the non-traited field. The dicamba concentrations measured by the Tisch air samplers in the north and east were also the highest among the sample locations.

In 2021, during the first week (July 7, 2021) assessment, the dicamba damage was level 2 in the north and west and level 1 in the east and south. The second week (July 14, 2021) showed level 2 damage in the north, south, and west and level 1 damage in the east. The third week (July 22, 2021) level 3 damage was observed in the south and west, level 2 dicamba damage was observed in the north, and level 1 in the east. In 2021, the onsite prevailing wind direction correlated with the observed dicamba damage in the northwest direction in the non-traited field. The dicamba concentrations measured by the Tisch samplers in the north and west were relatively high compared to the other sample locations.

In 2022, during the first week (July 4, 2022) assessment, in the west, north, and east directions, the dicamba damage at all distances (i.e., extending 15–45 m) was level 2, with minor leaf crinkling and stem twisting. In the south, there was no visible damage. The second week (July 11, 2022) assessments showed level 2 dicamba damage at 15 m, and level 1 damage at 30 and 45 m in all directions. In the third week (July 18, 2022) assessment, dicamba damage was level 3 at 15 m, level 2 at 30 m, and level 1 at 45 m in all directions. The visible symptoms included leaf deformation, moderate leaf cupping, and moderate stem twisting. During the fourth week (July 25, 2022), the dicamba damage in the west, north, and east between the border of the traited plot and 15 m distance showed level 4 damage. The symptoms progressed to severe deformation and death of the soybean plants. The damage at 30 m was level 2 in the north, east, and west. From the traited plot at 45 m, dicamba damage was level 1 and showed signs of recovery in the north, east, and west—similar recovery to that reported by Foster and Griffen (2018). In their study, they found that soybeans were able to recover from level 3 dicamba damage. During the fifth week (August 1, 2022), the dicamba damage in the north, east, and west was level 3 at 15 m, level 2 at 30 m, and level 1 at 45 m. The onsite prevailing wind direction correlated with the observed dicamba damage in the northwest and eastern directions in the non-traited field. The Tisch air samplers located in the north, west, and east revealed the highest dicamba concentrations (described later). Meteorological data and Tisch air sample data suggest that volatilization and transport post-spray were the main cause of the plant-related damage.

The non-traited soybean damage observed during these four experiments provides strong evidence for dicamba volatilization and transport after spray application. The dicamba-related plant damage indicates that current buffers and regulations specified for Minnesota are likely insufficient to prevent significant offsite damage. The current (as of 2022) label requirements for Minnesota include application before June 12 in the southern portion of the state and June 30 in the north, 29.4°C (85°F) air temperature limit, windspeeds under 4.4 m s^{-1} (10 mph), a general downwind buffer requirement of 73.2 m (240 ft), and the endangered species buffer requirement of 94.5 m (310 ft) (MDA, 2022).

Minnesota recorded 711 complaints in 2021, the highest number of reported dicamba damage incidents in the United States for the 2021 growing season (EPA, 2021). Notably, dicamba symptom expression often exhibits a time delay, influenced by various factors, including environmental conditions that significantly affect the recovery rate of soybeans. The offsite crop damage we documented in 2021 was consistent with the reported complaints filed with the Minnesota Department of Agriculture. We hypothesize that the extreme dry conditions in Minnesota in 2021 and 2022 decreased the ability of the non-traited soybean crop to recover from dicamba drift.

3.3 | Downwind dicamba concentrations

Table 3 reports the average dicamba concentrations for each experiment. In 2018 ($n = 5$ days), the average (± standard error) dicamba concentration was 0.72 ng m^{-3}. Day 1 had

TABLE 2 Dicamba flux (backward Lagrangian stochastic [bLS] calculated), meteorological conditions, and percentage loss of dicamba for each day and year of the experiment.

Date	Day of experiment	Flux (ng m^{-2} s^{-1})	Mean air temperature (°C)	Median atmospheric stability (*z*/*L*) (–)	Median wind speed (m s^{-1})	Median wind direction (°)	Mean relative humidity (%)	Dicamba loss (%)
2018								
June 14	0	0.004830	(D) 24.3	(D) −0.077	(D) 2.3	(D) 256	(D) 72.6	0.0750
			(N) 18.5	(N) 0.053	(N) 1.4	(N) 189	(N) 72.2	
June 15	1	0.513200	(D) 24.8	(D) −0.052	(D) 4.7	(D) 151	(D) 58.1	7.9180
			(N) 20.4	(N) 0.014	(N) 3.1	(N) 141	(N) 73.7	
June 16	2	0.000104	(D) 27.4	(D) −0.030	(D) 2.3	(D) 153	(D) 70.5	0.0016
			(N) 24.6	(N) 0.065	(N) 1.8	(N) 136	(N) 79.2	
June 17	3	0.000019	(D) 27.2	(D) −0.023	(D) 2.7	(D) 165	(D) 78.2	0.0003
			(N) 27.1	(N) 0.022	(N) 2.9	(N) 190	(N) 73.8	
June 18	4	0.000009	(D) 25.8	(D) −0.019	(D) 3.3	(D) 211	(D) 79.8	0.0001
			(N) 21.3	(N) 0.0030	(N) 2.1	(N) 92	(N) 97.7	
2019								
June 14	0	0.037060	(D) 20.4	(D) −0.071	(D) 2.5	(D) 101	(D) 71.2	0.5720
			(N) 16.4	(N) 0.0042	(N) 1.7	(N) 114	(N) 89.5	
June 17	1	0.053330	(D) 21.1	(D) −0.20	(D) 2.1	(D)286	(D) 60.2	0.8230
			(N) 16.4	(N) 0.074	(N) 0.8	(N) 270	(N) 78.9	
June 18	2	0.009694	(D) 21.3	(D) −0.28	(D) 2.5	(D) 297	(D) 52.1	0.1500
			(N) 14.4	(N) −0.15	(N) 0.4	(N) 276	(N) 88.6	
June 19	3	0.018080	(D) 22.1	(D) −0.15	(D) 3.0	(D) 68	(D) 53.3	0.2790
			(N) 17.4	(N) 0.066	(N) 1.1	(N) 43	(N) 73.7	
June 20	4	0.024800	(D) 16.7	(D) −0.080	(D) 2.5	(D) 148	(D) 92.8	0.3830
			(N) 15.7	(N) 0.040	(N) 1.4	(N) 107	(N) 96.9	
2021								
June 22	0	0.032430	(D) 21.5	(D)−0.13	(D) 1.7	(D) 142	(D) 42.3	0.5000
			(N) 15.4	(N) 0.063	(N) 1.0	(N) 109	(N) 73.3	
June 23	1	0.230800	(D) 27.0	(D) −0.093	(D) 2.9	(D) 147	(D) 59.0	3.5610
			(N) 25.4	(N) 0.033	(N) 2.7	(N) 172	(N) 72.4	
June 24	2	0.013650	(D) 28.3	(D) −0.065	(D) 2.6	(D) 306	(D) 57.5	0.2110
			(N)20.4	(N) 0.084	(N) 1.2	(N) 66	(N) 79.3	
June 25	3	0.046130	(D) 26.3	(D) −0.086	(D) 2.5	(D) 38	(D) 49.5	0.7120
			(N) 20.8	(N) 0.037	(N) 0.7	(N) 32	(N) 76.6	
June 26	4	0.009306	(D) 22.7	(D) −0.047	(D) 1.9	(D) 183	(D) 78.8	0.1440
			(N) 18.8	(N) 0.0061	(N) 0.7	(N) 196	(N) 89.3	

(Continues)

TABLE 2 (Continued)

Date	Day of experiment	Flux (ng m^{-2} s^{-1})	Mean air temperature (°C)	Median atmospheric stability (z/L) (–)	Median wind speed (m s^{-1})	Median wind direction (°)	Mean relative humidity (%)	Dicamba loss (%)
2022								
June 26	0	0.001812	(D) 21.0	(D) −0.023	(D) 4.6	(D) 301	(D) 41.4	0.0280
			(N) 15.1	(N) 0.0096	(N) 0.9	(N) 265	(N) 62.5	
June 27	1	1.797000	(D) 23.6	(D) −0.032	(D) 1.9	(D) 231	(D) 48.6	27.725
			(N) 19.2	(N) 0.0086	(N) 1.1	(N) 187	(N) 61.1	
June 28	2	0.006681	(D) 25.2	(D) −0.054	(D) 2.2	(D) 143	(D) 51.8	0.1030
			(N) 17.7	(N)0.073	(N) 1.4	(N) 24	(N) 78.4	
June 29	3	0.010550	(D) 27.2	(D) −0.015	(D) 3.7	(D) 158	(D) 54.9	0.1630
			(N)25.6	(N) 0.0233	(N) 3.5	(N) 182	(N) 60.7	
June 30	4	0.015560	(D) 25.5	(D) 0.023	(D) 2.1	(D) 197	(D) 61.7	0.2400
			(N) 20.6	(N) 0.066	(N) 1.0	(N) 324	(N) 63.8	

[a](D) represents daytime. (N) represents nighttime.

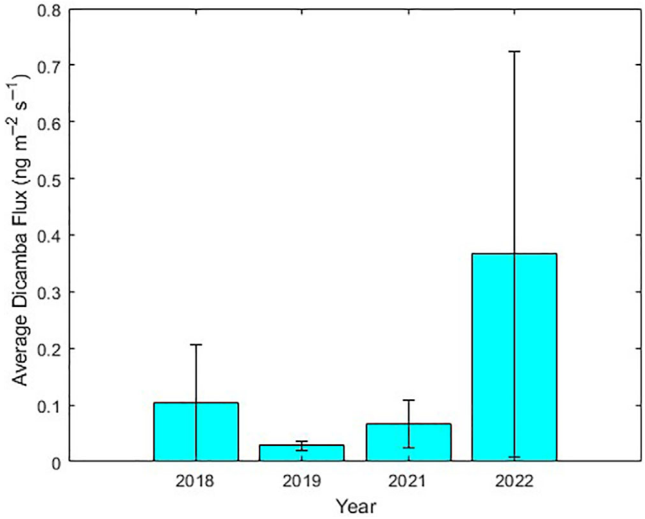

FIGURE 4 Average dicamba emissions estimated using the bLS approach. The error bars represent the standard error of the mean, with larger error bars arising due to high variability in daily dicamba concentrations.

the highest average dicamba concentration of 1.56 ng m^{-3}, presumably because drift during spray application made a significant offsite contribution to the measurement. The lowest dicamba concentrations were observed in 2019 ($n = 5$ days) with a mean concentration of 0.22 ng m^{-3}. Day 1 had the highest average dicamba concentration, 0.36 ng m^{-3}. In 2021 ($n = 5$ days), the average dicamba concentration was 0.31 ng m^{-3}. Day 1 had the highest average dicamba concentration of 1.00 ng m^{-3}. In 2022 ($n = 5$ days), the average dicamba concentration was 5.42 ng m^{-3}, yielding the highest observed concentrations when compared to all other years. Day 1 had the highest average dicamba concentration of 23.53 ng m^{-3}. For each year of the experiment (Table 3), dicamba concentrations were highest within the first 24 h of spray application, indicating significant drift and volatilization. The fact that dicamba concentrations were detected through the entire 5-day sampling period provides compelling evidence of volatilization and subsequent downwind transport following spray application.

3.4 | Dicamba emissions

The bLS emission estimates are shown in Figure 4 and Table S3. The average dicamba flux in 2018 (n = 5 days) was 0.10 ± 0.03 ng m^{-2} s^{-1}, representing approximately 8.0% of the dicamba spray that was applied. In 2018, the highest dicamba emissions, 0.51 ± 0.02 ng m^{-2} s^{-1}, occurred on day 1. The lowest average dicamba emissions were observed in 2019 ($n = 5$ days) with an average emission of 0.03 ± .001 ng m^{-2} s^{-1} with a total loss of 2.2% of applied spray. Day 1 had the highest emissions of 0.05 ± 0.002 ng m^{-2} s^{-1}. In

TABLE 3 Daily and seasonal average dicamba concentrations (mean ± standard error).

Year	Average dicamba concentration (ng m^{-3})					
	Day 0	Day 1	Day 2	Day 3	Day 4	Seasonal average
2018	0.14 ± 0.03	1.56 ± 0.42	1.37 ± 0.26	0.36 ± 0.05	0.16 ± 0.04	0.72 ± 0.12
2019	0.17 ± 0.02	0.36 ± 0.11	0.14 ± 0.02	0.20 ± 0.02	0.21 ± 0.10	0.22 ± 0.04
2021	0.02 ± 0.01	1.00 ± 0.45	0.25 ± 0.13	0.23 ± 0.13	0.04 ± 0.02	0.31 ± 0.18
2022	0.14 ± 0.03	23.5 ± 8.51	2.13 ± 0.60	1.04 ± 0.27	0.27 ± 0.08	5.42 ± 4.54

2021, the average emission ($n = 5$ days) was 0.07 ± 0.003 ng m^{-2} s^{-1}, representing a 5.1% loss of applied spray. Emissions were greatest, 0.23 ± 0.01 ng m^{-2} s^{-1}, on day 1. The highest emissions were observed in 2022. Average emissions ($n = 5$ days) were 0.37 ± 0.02 ng m^{-2} s^{-1}. The 5-day cumulative emissions represented approximately 28.3% of the spray application. Day 1 had the highest emissions, 1.80 ± 0.07 ng m^{-2} s^{-1}. The relatively large emissions during the first 24 h of each experiment indicates that application drift was a substantial component of the day 1 emissions. However, dicamba emissions were detected over the entire 5-day sampling period indicating that post-application volatilization was significant. These results are similar to the findings reported by Riter et al. (2020, 2021) and Sall et al. (2020), who detected significant dicamba emissions after spray application. However, their estimates were generally greater than the emissions reported here (Figures S4 and S5; Table S3).

Figures S4 and S5 and Table S3 present a comparison of dicamba estimates from previous studies (Riter et al., 2020, 2021; Sall et al., 2020) and this study, aiming to independently evaluate the magnitude of emissions, temporal variability, and the potential influence of measurement techniques. While all studies confirm significant offsite movement of dicamba following spray application, it is crucial to consider the variations in experimental conditions and methodologies that may have influenced the outcomes. Riter et al. (2020) conducted their experiment on two fields with areas of 1.62 and 4.05 ha, utilizing two different dicamba formulations (XtendiMax with Vaporgrip and Roundup Powermax) at a rate of 0.56 kg of dicamba per hectare. Their trials experienced air temperatures ranging from 22.3˚C to 35.3˚C, a maximum relative humidity of 58%, and wind speeds ranging from 1 to 4.5 m s^{-1}. In contrast, Sall et al. (2020) employed a 1.37-ha field, incorporating pH-buffers Clarity, XtendiMax, and Roundup Xtend at a relatively high application rate of 1.12 kg of dicamba per hectare. Their trials were characterized by air temperatures ranging from 14.1˚C to 31.4˚C, average relative humidity between 45.1% and 45.8%, and wind speeds ranging from 0.2 to 4.2 m s^{-1}. The relatively warmer and drier conditions in these studies compared to ours may explain the higher flux values observed. Additionally, differences in rate application, sampling time, plant growth phase, and measurement techniques could contribute to variations in the reported values. However, it is noteworthy that all of these studies identified day 1 as the period of highest dicamba emissions following application. Despite the reformulation of dicamba, utilization of pH-buffers, and regulatory adjustments, dicamba drift and volatility remains a significant factor contributing to downwind transport in all investigations. This emphasizes the necessity for further research and regulatory measures to mitigate the offsite movement of dicamba, even with the implementation of application guidelines.

3.5 | Constraints on downwind dicamba transport

We applied the fLS model to better understand the extent of downwind dicamba transport and to assess how atmospheric stability influenced downwind concentrations from day 2 of 2021 and 2022(Figures 5 and 6; Table S4). Figures 5 and 6 show that under stable conditions (slightly stable, moderately stable, and very stable) and neutral conditions, dicamba is likely to be transported further with higher average dicamba concentrations than in unstable (very unstable, moderately unstable, and slightly unstable) atmospheric conditions. Very stable atmospheric conditions have a higher probability of more dicamba particles traveling 100 m away from the target area. Similar results were reported by M. D. Bish, Farrell et al. (2019), who found that dicamba applied under unstable conditions resulted in less off-target movement. Our atmospheric modeling, constrained by concentration measurements, found that dicamba may be transported hundreds of meters under stable atmospheric conditions. However, this modeling approach does not explicitly account for dicamba chemical losses that occur during physical transport by turbulence. For example, dicamba is susceptible to photochemical degradation, particularly when in aqueous solution, on epicuticular waxes, in the presence of surfactants, and in formulation (Gruber et al., 2021). This implies that exposure to sunlight will lead to the breakdown of dicamba molecules, reducing its concentration in the atmosphere as it moves away from the point of origin. Further, Waite et al. (2002, 2005) have shown that dicamba undergoes both dry and wet

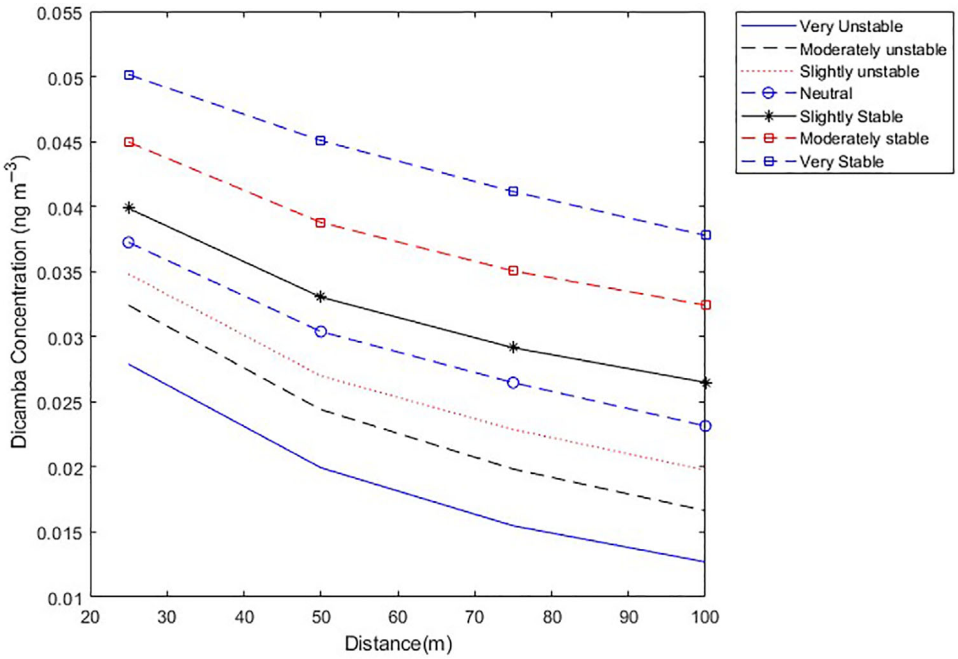

FIGURE 5 Estimating downwind dicamba concentration as a function of atmospheric stability. These simulations were constrained using flux estimates from day 2 of 2021. Simulations were performed using the forward Lagrangian stochastic (fLS) model in combination with 2021 data. Dicamba concentrations were estimated downwind at 25, 50, 75, and 100 m of the treated field for a broad range of atmospheric stabilities.

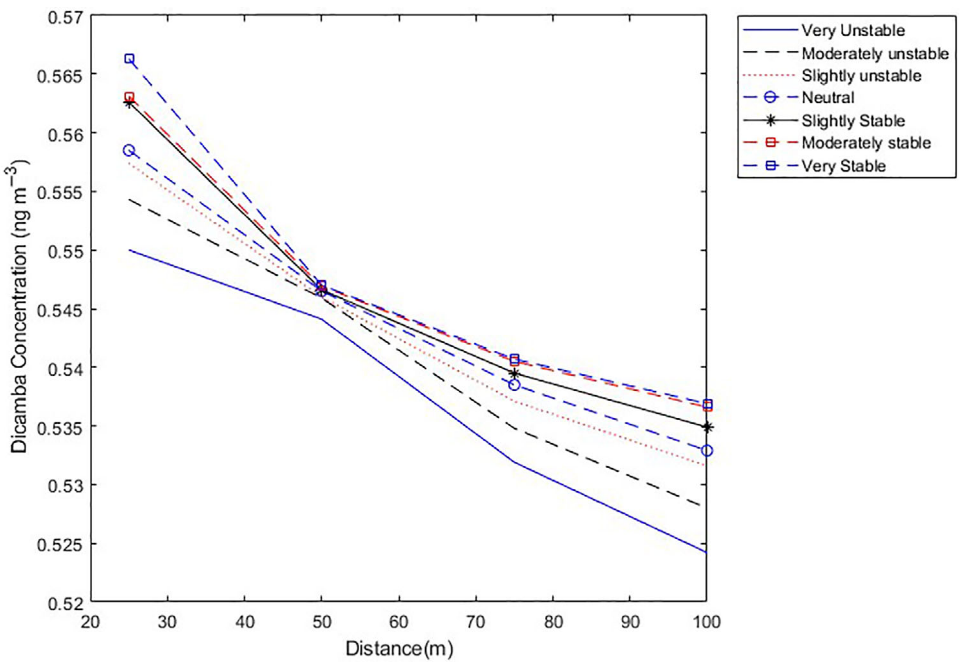

FIGURE 6 Estimating downwind dicamba concentration as a function of atmospheric stability. These simulations were constrained using initial flux estimates from day 2 of 2022. Simulations were performed using the forward Lagrangian stochastic (fLS) model in combination with 2022 data. Dicamba concentrations were estimated downwind at 25, 50, 75, and 100 m of the treated field for a broad range of atmospheric stabilities.

deposition, with higher deposition rates occurring close to local sources. Finally, the reaction of dicamba with hydroxyl radicals also contributes to faster photodegradation rates and a decrease in concentrations downwind from field sources (Gruber et al., 2021).

The analysis of daily data via ANOVA revealed that air temperature ($p = 0.043$) and wind speed ($p = 0.010$) significantly affected the variances of dicamba concentrations and fluxes. Regression analysis indicated that dicamba concentration was positively correlated to air

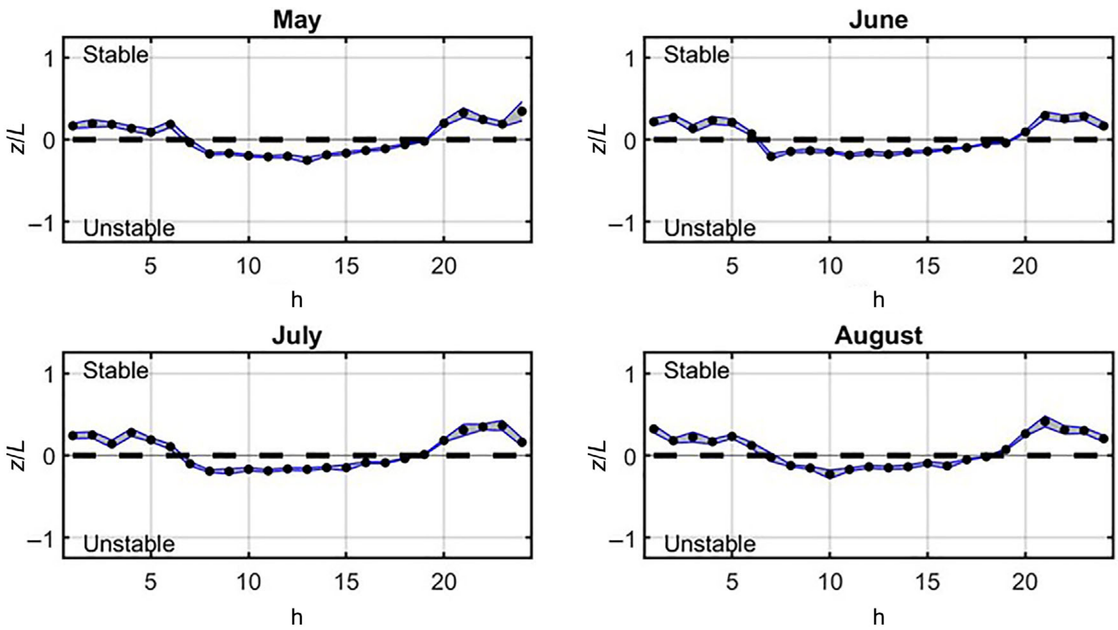

FIGURE 7 Diurnal ensemble variations in atmospheric stability measured using the eddy covariance approach at the Rosemount AmeriFlux site. Twenty site-years of data (corn/soybean) were used to estimate the average hourly ensemble for each month. The heavy dashed line shows the neutral atmospheric stability.

temperature (slope = 0.55 ng m^{-3}°C^{-1}, $r = 0.48$, $p = 0.043$) and wind speed (slope = 1.03 ng m^{-4} s, $r = 0.59$, $p = 0.010$). This supports the findings of R. Behrens and Lueschen (1979), who found that dicamba volatility decreased as temperature decreased. Further, Mueller and Steckel (2019) detected greater dicamba volatility at higher air temperatures. Wind speed is also known to affect dicamba off-target movement (Oslend et al., 2020; Sousa et al., 2017). Their work showed that lower wind speeds reduced the dispersion of dicamba over the target fields while relatively high wind speeds increased off-target movement of dicamba. This evidence reinforces the argument that air temperature and wind speed are key meteorological factors influencing dicamba volatilization and off-target movement (M. D. Bish, Farrell, et al., 2019; M. D. Bish, Guinan, et al., 2019; Egan & Mortensen, 2012; Grint & Werle, 2021).

Temperatures at or exceeding 30°C (86˚F), stable atmospheric conditions, and low wind speeds less than 1.47 m s^{-1} (3 mph) are likely to increase offsite soybean injury from dicamba volatilization (Grint & Werle, 2021). Further, high relative humidity (>85%) and rainfall events have been linked to reduced volatilization and injury to soybeans (R. Behrens & Lueschen, 1979; Zaccaro-Gruener et al., 2023). In 2022, we observed the highest dicamba emissions. The low relative humidity (<70%), high air temperatures, and drought-like conditions likely increased dicamba emissions. In experimental year 2018, dicamba emissions were relatively low, likely because of the relatively cool and wet conditions. When possible, it is recommended that dicamba application be reduced under drought-like conditions.

The 20 site-years of atmospheric stability, wind speed, and air temperature above crop surfaces at UMORE park (Rosemount, MN) indicate that there is a very limited window of time when it is safe (i.e., meeting current label requirements) to apply dicamba (Figures 7–9). For instance, stable atmospheric conditions persist over much of the growing season from about 7 p.m. to 8 a.m. and mean daytime wind speeds approach 4.44 m s^{-1} (i.e., label cutoff requirement) from mid to late afternoon during spring. The application of spray under unstable atmospheric conditions with relatively low wind speed and low surface temperature can reduce potential drift but can be difficult to achieve, considering typical meteorological conditions over agricultural sites in the Upper Midwest.

4 | CONCLUSIONS

Dicamba was reformulated to reduce volatility and off-target movement. Despite this reformulation, we found that dicamba was susceptible to drift and volatilization with continuous emissions observed over each of the 5-day sampling period. The highest movement of dicamba through spray drift and volatilization occurred on the day of application. However, the post-spray dicamba volatilization and downwind transport was significant and posed a risk to nontarget crops. The existing label and recommended buffers for dicamba addressed volatilization and drift during application but not post-application volatilization. Based on our findings, reinforcing dicamba application restrictions, particularly targeting

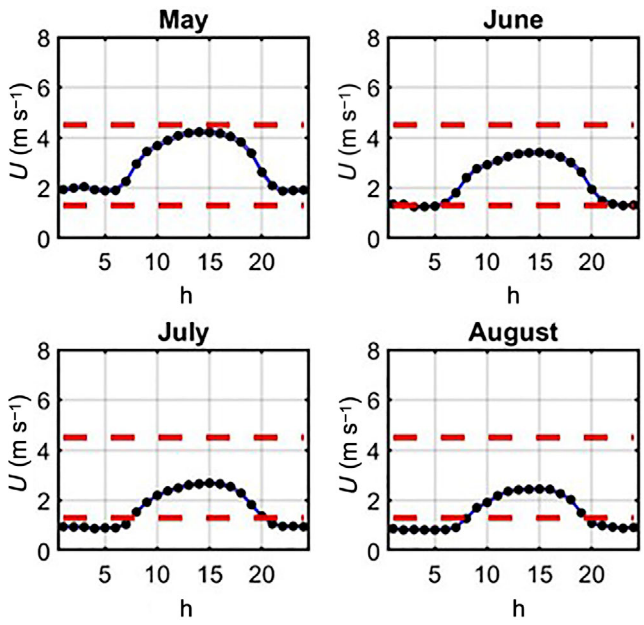

FIGURE 8 Diurnal ensemble variations in wind speed measured with the eddy covariance approach at the Rosemount AmeriFlux site. Twenty site-years of data (corn/soybean) were used to estimate the average hourly ensemble for each month. The heavy dashed line shows the minimum and maximum acceptable wind speed thresholds for dicamba spray application.

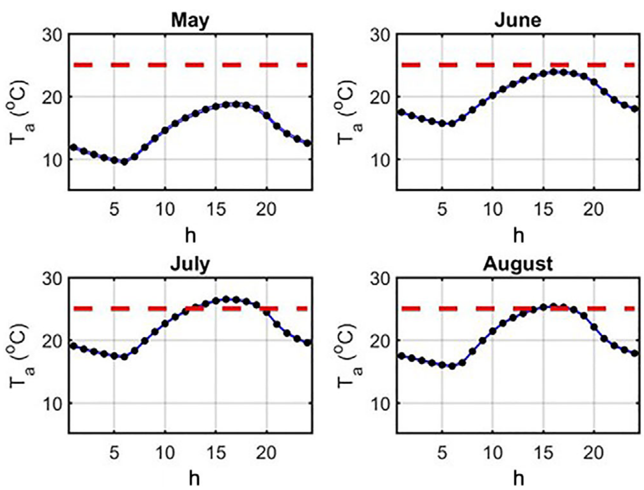

FIGURE 9 Diurnal ensemble variations in air temperature measured at the Rosemount AmeriFlux site. Twenty site-years of data (corn/soybean) were used to estimate the average hourly ensemble for each month. The heavy dashed line shows the maximum acceptable air temperature threshold for dicamba spray application.

post-application volatilization, is recommended. For example, continuous off-target movement of dicamba beyond 24 h indicates the need for buffers designed for post-application scenarios. Additionally, it is recommended to consider reduced application or stringent precautions during dry periods in affected regions.

AUTHOR CONTRIBUTIONS

Caleb R. Hammer: Data curation; formal analysis; investigation; methodology; writing—original draft; writing—review and editing. **Timothy J. Griffis**: Conceptualization; data curation; funding acquisition; methodology; project administration; resources; supervision; validation; visualization; writing—original draft; writing—review and editing. **John M. Baker**: Conceptualization; methodology; resources; visualization; writing—review and editing. **Pamela J. Rice**: Conceptualization; methodology; resources; supervision; visualization; writing—review and editing. **Lara E. Frankson**: Data curation; formal analysis; investigation; methodology; resources; writing—review and editing. **Jeffrey L. Gunsolus**: Conceptualization; writing—review and editing. **Matthew D. Erickson**: Data curation; investigation; methodology. **Ke Xiao**: Formal analysis; investigation; writing—original draft; writing—review and editing. **Aarti P. Mistry**: Data curation; formal analysis; writing—original draft; writing—review and editing. **Debalin Sarangi**: Conceptualization.

ACKNOWLEDGMENTS

The authors would like to thank William Breiter, Cody Winker, Anna Andresen, Emilee Brandt, Jennifer Hamlin, Ed Joice, Christopher Sanchez, Joe Schleiss, Claire Simmerman, Eric Verbeke, and Blake Webster for their help with the field experiments and data acquisition. Mention of trade names or commercial products in this publication is solely for the purpose of providing specific information and does not imply recommendation or endorsement by the U.S. Department of Agriculture. The U.S. Department of Agriculture (USDA) prohibits discrimination in all its programs and activities on the basis of race, color, national origin, age, disability, and where applicable, sex, marital status, familial status, parental status, religion, sexual orientation, genetic information, political beliefs, reprisal, or because all or part of an individual's income is derived from any public assistance program. (Not all prohibited bases apply to all programs.) Persons with disabilities who require alternative means for communication of program information (Braille, large print, audiotape, etc.) should contact USDA's TARGET Center at (202) 720-2600 (voice and TDD). To file a complaint of discrimination, write to USDA, Director, Office of Civil Rights, 1400 Independence Avenue, S.W., Washington, D.C. 20250-9410, or call (800) 795-3272 (voice) or (202) 720-6382 (TDD). USDA is an equal opportunity provider and employer. USDA is an equal opportunity provider and employer. This research was supported by the University of Minnesota Rapid Agricultural Response Fund, the Minnesota Department of Agriculture, the USDA Agricultural Research Service, and US Department of Energy AmeriFlux Core Site Program.

CONFLICT OF INTEREST STATEMENT

The authors declare no conflicts of interest.

ORCID

Caleb R. Hammer https://orcid.org/0009-0003-7945-1006

REFERENCES

Andrilenas, P. A. (1974). *Farmers' use of pesticides in 1971: Quantities* (AER-252). USDA-ERS. https://naldc.nal.usda.gov/catalog/CAT85826968

Balkema, G., & Pancheva, E. (2016). Power limits for central order statistics: I. Continuous limit laws. *Extremes*, *20*(1), 91–110. https://doi.org/10.1007/s10687-016-0265-1

Baker, J. M., & Griffis, T. J. (2005). Examining strategies to improve the carbon balance of corn/soybean agriculture using eddy covariance and mass balance techniques. *Agricultural and Forest Meteorology*, *128*, 163–177. https://doi.org/10.1016/j.agrformet.2004.11.005

Batts, T. M., Miller, D. K., Griffin, J. L., Villordon, A. O., Stephenson, D. O., Jennings, K. M., Chaudhari, S., Blouin, D. C., Copes, J. T., & Smith, T. P. (2021). Impact of reduced rates of dicamba and glyphosate on sweetpotato growth and yield. *Weed Technology*, *35*(1), 27–34. https://doi.org/10.1017/wet.2020.54

Behrens, M. R., Mutlu, N., Chakraborty, S., Dumitru, R., Jiang, W. Z., LaVallee, B. J., Herman, P. L., Clemente, T. E., & Weeks, D. P. (2007). Dicamba resistance: Enlarging and preserving biotechnology-based weed management strategies. *Science*, *316*(5828), 1185–1188. https://doi.org/10.1126/science.1141596

Behrens, R., & Lueschen, W. E. (1979). Dicamba volatility. *Weed Science*, *27*(5), 486–493. https://doi.org/10.1017/S0043174500044453

Bish, M., Oseland, E., & Bradley, K. (2021). Off-target pesticide movement: A review of our current understanding of drift due to inversions and secondary movement. *Weed Technology*, *35*(3), 345–356. https://doi.org/10.1017/wet.2020.138

Bish, M. D., Farrell, S. T., Lerch, R. N., & Bradley, K. W. (2019). Dicamba losses to air after applications to soybean under stable and nonstable atmospheric conditions. *Journal of Environmental Quality*, *48*(6), 1675–1682. https://doi.org/10.2134/jeq2019.05.0197

Bish, M. D., Guinan, P. E., & Bradley, K. W. (2019b). Inversion climatology in high-production agricultural regions of Missouri and implications for pesticide applications. *Journal of Applied Meteorology and Climatology*, *58*(9), 1973–1992. https://doi.org/10.1175/JAMC-D-18-0264.1

Carbonari, C. A., Costa, R. N., Giovanelli, B. F., Bevilaqua, N. C., Palhano, M., Barbosa, H., Lopez Ovejero, R. F., & Velini, E. D. (2022). Volatilization of dicamba diglycolamine salt in combination with glyphosate formulations and volatility reducers in Brazil. *Agronomy*, *12*(5), 1001. https://doi.org/10.3390/agronomy12051001

Castner, M., Norsworthy, J. K., Barber, T., Roberts, T. L., & Gbur, E. (2022). Effect of dicamba on reproductive development in corn and rice. *Agrosystems, Geosciences & Environment*, *5*(1), e20256. https://doi.org/10.1002/agg2.20256

Da Silva, A., Sinfort, C., Tinet, C., Pierrat, D., & Huberson, S. (2006). A Lagrangian model for spray behaviour within vine canopies. *Journal of Aerosol Science*, *37*(5), 658–674. https://doi.org/10.1016/j.jaerosci.2005.05.016

Dintelmann, B. R., Farrell, S. T., & Bradley, K. W. (2022). Influence of recovery treatments on dicamba-injured soybean. *Weed Technology*, *36*(1), 1–7. https://doi.org/10.1017/wet.2021.63

Egan, J. F., & Mortensen, D. A. (2012). Quantifying vapor drift of dicamba herbicides applied to soybean. *Environmental Toxicology and Chemistry*, *31*(5), 1023–1031. https://doi.org/10.1002/etc.1778

EPA. (2017). *Dicamba—Method GRM022.08A for the determination of dicamba from air sampling tube and filter paper by LC-MS/MS* (EPA 850.6100). Environmental Protection Agency. https://www.epa.gov/sites/default/files/2020-09/documents/ecm-dicamba_in_air-mrid_50102120.pdf

EPA. (2021). *Status of over-the-top dicamba: Summary of 2021 usage, incidents and consequences of off-target movement, and impacts of stakeholder-suggested mitigations* (DP# 464173: PC Code 128931). Environmental Protection Agency. https://www.regulations.gov/document/EPA-HQ-OPP-2020-0492-0021

EPA. (2022). *DICAMBA HD 5*. https://www3.epa.gov/pesticides/chem_search/ppls/045002-00039-20220425.pdf

EPA. (2023). Registration of *dicamba for use on dicamba-tolerant crops*. Environmental Protection Agency. https://www.epa.gov/ingredients-used-pesticide-products/registration-dicamba-use-dicamba-tolerant-crops

Flesch, T., Prueger, J. H., & Hatfield, J. L. (2002). Turbulent Schmidt number from a tracer experiment. *Agricultural and Forest Meteorology*, *111*, 299–307. https://doi.org/10.1016/S0168-1923(02)00025-4

Flesch, T. K., & Aylor, D. E. (2000). *A Lagrangian stochastic dispersion model for assessing pesticide spray drift in an Orchard canopy*. Connecticut Agricultural Experiment Station.

Flesch, T. K., & Wilson, J. D. (2015). Estimating tracer emissions with a backward Lagrangian stochastic technique. In J. L. Hatfield & J. M. Baker (Eds.), *Micrometeorology in agricultural systems* (Vol. 47, pp. 513–531). ASA, CSSA, SSSA. https://doi.org/10.2134/agronmonogr47.c22

Forster, M. R., & Griffen, J. L. (2018). Injury criteria associated with soybean exposure to dicamba. *Weed Technology*, *32*(5), 608–617. https://doi.org/10.1017/wet.2018.42

Government of Canada. (2022). *Guidelines for Canadian drinking water quality: Dicamba guideline technical document*. https://www.canada.ca/en/health-canada/services/publications/healthy-living/guidelines-canadian-drinking-water-quality-guideline-technical-document-dicamba.html#a50

Grint, K., & Werle, R. (2021). *Understanding dicamba volatility*. Nutrient and Pest Management (NPM) Program. https://richland.extension.wisc.edu/files/2021/12/Understanding-Dicamba-Volatility.pdf

Gruber, K., Courteau, B., Bokhoree, M., McMahon, E., Kotz, J., & Nienow, A. (2021). Photolysis of the herbicide dicamba in aqueous solutions and on corn (*Zea mays*) epicuticular waxes. *Environmental Science: Processes & Impacts*, *23*(5), 786–802. https://doi.org/10.1039/D1EM00058F

Hartzler, B. (2017a). Dicamba: Past, present, and future. In *Proceedings of the integrated crop management conference* (pp. 11173819). Iowa State University. https://doi.org/10.31274/icm-180809-241

Hartzler, B. H. (2017b). *Factors influencing dicamba volatility*. Iowa State University Extension and Outreach. https://crops.extension.iastate.edu/blog/bob-hartzler/factors-influencing-dicamba-volatility

Huang, H., & Li, X. (2023). A theoretical model for structure inclination angles in stratified boundary layers: Connecting turbulent scaling and Monin–Obukhov similarity theory. *AIP Advances*, *13*(8), 085326. https://doi.org/10.1063/5.0159628

IDOA. (2024). *Dicamba*. https://agr.illinois.gov/pesticides/dicamba.html#:~:text=A%20pesticide%20containing%20dicamba%20shall

Jha, P. (2023). *New cut-off date for over-the-top dicamba use in Iowa for 2023*. Iowa State University. https://crops.extension.iastate.edu/blog/prashant-jha/new-cut-date-over-top-dicamba-use-iowa-2023#:~:text=For%20the%202023%20season%2C%20the

Jones, G. T., Norsworthy, J. K., Barber, T., Gbur, E., & Kruger, G. R. (2019). Off-target movement of DGA and BAPMA dicamba to sensitive soybean. *Weed Technology*, *33*(1), 51–65. https://doi.org/10.1017/wet.2018.121

Marques, M. G., da Cunha, J. P. A. R., & Lemes, E. M. (2021). Dicamba injury on soybean assessed visually and with spectral vegetation index. *AgriEngineering*, *3*(2), 240–250. https://doi.org/10.3390/agriengineering3020016

McCown, S., Barber, T., & Norsworthy, J. K. (2018). Response of non–dicamba-resistant soybean to dicamba as influenced by growth stage and herbicide rate. *Weed Technology*, *32*(5), 513–519. https://doi.org/10.1017/wet.2018.64

MDA. (2019). *Dicamba new use review* (CAS 104040-79-1; EPA PC Code 128931). Minnesota Department of Agriculture. https://www.mda.state.mn.us/sites/default/files/inline-files/dicambatier1.pdf

MDA. (2022). *EPA approves 2022 Minnesota-specific restrictions for dicamba herbicide*. MDA, Minnesota Department of Agriculture. https://www.mda.state.mn.us/epa-approves-2022-minnesota-specific-restrictions-dicamba-herbicide

MDARD. (2024). *Restricted use pesticides dealers in Michigan*. https://www.michigan.gov/mdard/licensing/pesticide/rup

Meyeres, T., Lancaster, S., Kumar, V., Roozeboom, K., & Peterson, D. (2021). Response of non-dicamba-resistant soybean (*Glycine max*) varieties to dicamba. *Weed Technology*, *35*(5), 718–724. https://doi.org/10.1017/wet.2021.4

Meyeres, T., Lancaster, S., Kumar, V., Roozeboom, K., & Peterson, D. (2022). Non-dicamba-resistantsoybean response to multiple dicamba applications. *Agronomy Journal*, *115*(1), 147–160. https://doi.org/10.1002/agj2.21201

Mueller, T. C., & Steckel, L. E. (2019). Dicamba volatility in humidomes as affected by temperature and herbicide treatment. *Weed Technology*, *33*(4), 541–546. https://doi.org/10.1017/wet.2019.36

Mueller, T. C., & Steckel, L. E. (2021). Dicamba emissions under field conditions as affected by surface condition. *Weed Technology*, *35*(2), 188–195. https://doi.org/10.1017/wet.2020.106

OISC. (2023). *2023 Dicamba: Frequently asked questions*. https://oisc.purdue.edu/pesticide/dicamba.html

Oke, T. R. (1987). *Boundary layer climates* (2nd ed.). Routledge. https://doi.org/10.4324/9780203407219

Oseland, E., Bish, M., Steckel, L., & Bradley, K. (2020). Identification of environmental factors that influence the likelihood of off-target movement of dicamba. *Pest Management Science*, *76*(9), 3282–3291. https://doi.org/10.1002/ps.5887

Prueger, J. H., & Kustas, W. P. (2015). Aerodynamic methods for estimating turbulent fluxes. In J. L. Hatfield & J. M. Baker (Eds.), *Agronomy monographs* (pp. 407–436). ASA, CSSA, SSSA. https://doi.org/10.2134/agronmonogr47.c18

R Core Team. (2021). *R: A language and environment for statistical computing* (R version 4.0.2) [Computer software]. R Foundation for Statistical Computing. https://www.R-project.org

Riter, L. S., Pai, N., Vieira, B. C., MacInnes, A., Reiss, R., Hapeman, C. J., & Kruger, G. R. (2021). Conversations about the future of dicamba: The science behind off-target movement. *Journal of Agricultural and Food Chemistry*, *69*(48), 14435–14444. https://doi.org/10.1021/acs.jafc.1c05589

Riter, L. S., Sall, E. D., Pai, N., Beachum, C. E., & Orr, T. B. (2020). Quantifying dicamba volatility under field conditions: Part I, methodology. *Journal of Agricultural and Food Chemistry*, *68*(8), 2277–2285. https://doi.org/10.1021/acs.jafc.9b06451

Robinson, A. P., Simpson, D. M., & Johnson, W. G. (2013). Response of glyphosate-tolerant soybean yield components to dicamba exposure. *Weed Science*, *61*(4), 526–536. https://doi.org/10.1614/WS-D-12-00203.1

Sall, E. D., Huang, K., Pai, N., Schapaugh, A. W., Honegger, J. L., Orr, T. B., & Riter, L. S. (2020). Quantifying dicamba volatility under field conditions: Part II, comparative analysis of 23 dicamba volatility field trials. *Journal of Agricultural and Food Chemistry*, *68*(8), 2286–2296. https://doi.org/10.1021/acs.jafc.9b06452

Sciumbato, A. S., Chandler, J. M., Senseman, S. A., Bovey, R. W., & Smith, K. L. (2004). Determining exposure to auxin-like herbicides. I. Quantifying injury to cotton and soybean. *Weed Technology*, *18*(4), 1125–1134. https://doi.org/10.1614/WT-03-105R1

Shapiro, S., & Wilk, M. (1965). An analysis of variance test for normality (complete samples). *Biometrika*, *52*(3/4), 591–611. https://doi.org/10.2307/2333709

Soltani, N., Oliveira, M. C., Alves, G. S., Werle, R., Norsworthy, J. K., Sprague, C. L., Young, B. G., Reynolds, D. B., Brown, A., & Sikkema, P. H. (2020). Off-target movement assessment of dicamba in North America. *Weed Technology*, *34*(3), 318–330. https://doi.org/10.1017/wet.2020.17

Sousa Alves, G., Kruger, G. R., da Cunha, J. P. A. R., de Santana, D. G., Pinto, L. A. T., Guimarães, F., & Zaric, M. (2017). Dicamba spray drift as influenced by wind speed and nozzle type. *Weed Technology*, *31*(5), 724–731. https://doi.org/10.1017/wet.2017.61

Stull, R. B. (1988). *An introduction to boundary layer meteorology*. Kluwer Academic Publishers.

Tomasko, S. (2022). *Dicamba use for soybeans: No rule changes for 2023*. University of Wisconsin Pesticide Applicator Training Program. https://fyi.extension.wisc.edu/pat/2022/11/21/dicamba-use-for-soybeans-no-rule-changes-for-2023/

Waite, D. T., Bailey, P., Sproull, J. F., Quiring, D. V., Chau, D. F., Bailey, J., & Cessna, A. J. (2005). Atmospheric concentrations and dry and wet deposits of some herbicides currently used on the Canadian Prairies. *Chemosphere*, *58*(6), 693–703. https://doi.org/10.1016/j.chemosphere.2004.09.105

Waite, D. T., Sproull, J. F., Quiring, D. V., & Cessna, A. J. (2002). Dry atmospheric deposition and deposition velocities of dicamba, 2,4-dichlorophenoxyacetic acid and γ-1,2,3,4,5,6-hexachlorocyclohexane. *Analytica Chimica Acta*, *467*(1–2), 245–252.

Zaccaro-Gruener, M. L., Norsworthy, J. K., Brabham, C. B., Barber, L. T., Butts, T. R., Roberts, T. L., & Mauromoustakos, A. (2022). Evaluation of dicamba volatilization when mixed with glyphosate using imazethapyr as a tracer. *Journal of Environmental Management*, *317*, 115303. https://doi.org/10.1016/j.jenvman.2022.115303

Zaccaro-Gruener, M. L., Norsworthy, J. K., Brabham, C. B., Barber, L. T., Roberts, T. L., Mauromoustakos, A., & Mueller, T. C. (2023). Dicamba air concentrations in eastern Arkansas and impact on soybean. *Weed Science*, *71*(3), 265–277. https://doi.org/10.1017/wsc.2023.22

SUPPORTING INFORMATION

Additional supporting information can be found online in the Supporting Information section at the end of this article.

How to cite this article: Hammer, C. R., Griffis, T. J., Baker, J. M., Rice, P. J., Frankson, L. E., Gunsolus, J. L., Erickson, M. D., Xiao, K., Mistry, A. P., & Sarangi, D. (2024). Reformulation of dicamba herbicide: Impacts on offsite transport and soybean damage. *Agronomy Journal*, *116*, 2200–2216. https://doi.org/10.1002/agj2.21630